Clinical Cancer Research

Fractionated Dosing Improves Preclinical Therapeutic Index of Pyrrolobenzodiazepine-Containing Antibody Drug Conjugates

Mary Jane Masson Hinrichs[1], Pauline M. Ryan[1], Bo Zheng[2], Shameen Afif-Rider[1], Xiang Qing Yu[2], Michele Gunsior[2], Haihong Zhong[3], Jay Harper[3], Binyam Bezabeh[4], Kapil Vashisht[1], Marlon Rebelatto[1], Molly Reed[1], Patricia C. Ryan[1], Shannon Breen[3], Neki Patel[5], Cui Chen[3], Luke Masterson[5], Arnaud Tiberghien[5], Phillip W. Howard[5], Nazzareno Dimasi[4], and Rakesh Dixit[1]

Abstract

Purpose: To use preclinical models to identify a dosing schedule that improves tolerability of highly potent pyrrolobenzodiazepine dimers (PBDs) antibody drug conjugates (ADCs) without compromising antitumor activity.

Experimental Design: A series of dose-fractionation studies were conducted to investigate the pharmacokinetic drivers of safety and efficacy of PBD ADCs in animal models. The exposure–activity relationship was investigated in mouse xenograft models of human prostate cancer, breast cancer, and gastric cancer by comparing antitumor activity after single and fractionated dosing with tumor-targeting ADCs conjugated to SG3249, a potent PBD dimer. The exposure–tolerability relationship was similarly investigated in rat and monkey toxicology studies by comparing tolerability, as assessed by survival, body weight, and organ-specific toxicities, after single and fractionated dosing with ADCs conjugated to SG3249 (rats) or SG3400, a structurally related PBD (monkeys).

Results: Observations of similar antitumor activity in mice treated with single or fractionated dosing suggests that antitumor activity of PBD ADCs is more closely related to total exposure (AUC) than peak drug concentrations (C_{max}). In contrast, improved survival and reduced toxicity in rats and monkeys treated with a fractionated dosing schedule suggests that tolerability of PBD ADCs is more closely associated with C_{max} than AUC.

Conclusions: We provide the first evidence that fractionated dosing can improve preclinical tolerability of at least some PBD ADCs without compromising efficacy. These findings suggest that preclinical exploration of dosing schedule could be an important clinical strategy to improve the therapeutic window of highly potent ADCs and should be investigated further. *Clin Cancer Res; 23(19); 5858–68. ©2017 AACR.*

Introduction

Antibody drug conjugates (ADCs) are a rapidly growing class of targeted anticancer therapeutics that now account for a significant fraction of pharmaceutical pipelines (1). Much of the interest in this technology stems from the recent marketing approvals of ado-trastuzumab emtansine (Kadcyla) for the treatment of metastatic breast cancer and brentuximab vedotin (Adcetris) for the treatment of Hodgkin's lymphoma. Despite the success of the two marketed products, clinical development of ADCs continues to be impeded by inability to escalate to dosage range expected to achieve desired therapeutic effects due to safety issues (2). Of the greater than 50 ADCs evaluated in early clinical trials, approximately 20 have been discontinued due to lack of efficacy and/or intolerable toxicity (3). Optimizing dosing schedule could be an important strategy to decrease adverse events while maintaining exposure and efficacy (4). Doing so requires a greater understanding of the relationship between exposure and toxicity in order to inform the clinical dosing schedule. The most common clinical dosing schedule for ADCs is every 3 weeks (3). This schedule results in high peak plasma concentrations with minimal-to-no accumulation with repeated dosing (5). Although every 3 weeks dosing is consistent with dosing schedules used for most chemotherapy regimens, it is unclear whether this represents the ideal dosing regimen for ADCs. In addition, there is very limited clinical data available to examine the potential benefits of alternative dosing schedules (3, 6, 7). SAR3419, an anti-CD19 ADC conjugated to the maytansinoid DM4, is an example where use of alternative dosing schedule positively impacted clinical development of an ADC. In the first in human trial, the maximum tolerated dose (MTD) was 160 mg/m^2 on a every 3 weeks dosing schedule (8). Although the overall response rate (ORR)

[1]Biologics Safety Assessment, MedImmune, Gaithersburg, Maryland. [2]Clinical Pharmacology and DMPK, MedImmune, Gaithersburg, Maryland. [3]Oncology Research, MedImmune, Gaithersburg, Maryland. [4]Antibody Discovery and Protein Engineering, MedImmune, Gaithersburg, Maryland. [5]Spirogen Ltd., QMB Innovation Centre, London, United Kingdom.

Note: Supplementary data for this article are available at Clinical Cancer Research Online (http://clincancerres.aacrjournals.org/).

M.J.M. Hinrichs and P.M. Ryan contributed equally to this article.

Corresponding Author: Mary Jane Masson Hinrichs, MedImmune LLC, 1 MedImmune Way, Gaithersburg, MD 20878. Phone: 2022957576; Fax: 3013981111; E-mail: hinrichsm@medimmune.com

doi: 10.1158/1078-0432.CCR-17-0219

Translational Relevance

Optimization of dosing schedule could be an important mitigation strategy to improve tolerability of ADCs with narrow therapeutic windows, especially those conjugated to highly potent payloads such as pyrrolobenzodiazepine dimers (PBDs). Doing so requires a greater understanding of the exposure–response relationship to enable selection of a dosing regimen that decreases adverse events while maintaining efficacy. Assessing this relationship in patients can be lengthy and resource intensive; therefore, we evaluated whether preclinical models could be used to understand the pharmacokinetic drivers of safety and efficacy for PBD ADCs in animals. By conducting a series of dose-fractionation studies, we determined that fractionated dosing improved tolerability of PBD ADCs without impacting antitumor activity. Together, these results suggest that fractionated dosing could widen the therapeutic window of PBD ADCs.

at this dose level was 22%, findings of grade 2/3 ocular toxicity prevented escalation to higher, potentially more efficacious dose levels (9). In an attempt to improve tolerability, a fractionated dose schedule was evaluated in which patients were administered four weekly doses of 55 mg/m^2 followed by four additional doses every 2 weeks. Use of this schedule appeared to have a positive impact as the ORR increased to 33%, and the severity of ocular toxicity decreased to mostly grade 1 events. Despite the success with SAR3419, reports with other ADCs have been mixed. In the case of gemtuzumab ozogamicin (Mylotarg), an anti-CD33 antibody conjugated to calicheamicin, early data from a multicenter phase II uncontrolled trial in 57 adult patients with acute myeloblastic leukemia (AML), patients demonstrated that fractionated dosing with monotherapy Mylotarg significantly improved safety without impacting efficacy (10). However, follow-up data from a small retrospective study in relapsed/refractory patients with AML treated with Mylotarg in combination with chemotherapy, using either the standard every 3 weeks (18 patients) or a fractionated (15 patients) dosing schedule, failed to demonstrate significant differences in outcomes or safety between the two schedules (11, 12). Although these data demonstrate that alternative dosing regimens do not always improve the therapeutic index of ADCs, it is clear that further exploration of the relationship is warranted given the high attrition rate of clinical stage ADCs.

Recently, there has been significant interest in developing next-generation ADCs with increased potency and alternative mechanisms of action. Pyrrolobenzodiazepine dimers (PBDs) are a class of DNA crosslinking warheads that are significantly more potent than the tubulin-inhibiting payloads used in most clinical-phase ADCs (13). Interest in PBD dimers has grown significantly over the past year following the release of promising clinical data from trials with PBD conjugates, rovalpituzumab tesirine (14) and vadastuximab talirine (SGN-CD33A; ref. 15), in difficult-to-treat cancers, such as small cell lung cancer and relapsed, refractory acute myeloid leukemia, respectively. As a result, it is anticipated that a significant number of PBD ADCs will advance into clinical development over the next few years. Although increased potency can enhance the antitumor activity of an ADC, it also increases the risk of safety issues due to steep dose–response curves. Therefore, understanding the relationship between exposure and tolerability is essential to selecting a rational dosing schedule. We conducted a series of preclinical safety and efficacy studies to better understand the relationship between exposure and therapeutic index of PBD ADCs. Our aim was to identify whether dosing schedule can improve tolerability of highly potent ADC without compromising antitumor activity.

Materials and Methods

Test articles

The anti-EphA2 (1C1), anti-5T4 (5T4), and isotype control (R347) antibodies used in these studies have been previously described (16–18). 1C1 cross-reacts with rat, monkey, and human EphA2; 5T4 is only cross-reactive with monkey and human 5T4 (16, 19). These antibodies were engineered to enable site-specific conjugation of two PBD dimers per antibody. The maleimide-PEG8 PBD dimers used for conjugation were SG3249, also known as tesirine (20), and SG3400, a PBD dimer based on SG2000 (21, 22). Site-specific conjugation was carried out as described previously (17). Briefly, antibodies were reduced using 40 molar equivalents of Tris (2-carboxy-ethyl)-phosphine (TCEP) in PBS pH 7.2, 1 mmol/L ethylenediamine tetraaceticacid (EDTA) for 3 hours at 37°C. Following overnight dialysis in PBS pH 7.2, 1 mmol/L EDTA at 4°C using 10,000 MWCO dialysis cassettes, 20 molar equivalents of dehydroascorbic acid were added for 4 hours at 25°C. The solution was filtered through a 0.2-μm syringe filter and eight equivalents of SG3249 or SG3400 were sequentially added, followed by incubation at room temperature for 1 hour under gentle rotation. The conjugation was quenched by the addition of 4 molar equivalents (over SG3249 or SG3400) of N-acetyl cysteine. Free unreacted SG3249 and SG3400 and macromolecular aggregates were removed using ceramic hydroxyapatite type II chromatography as described previously (18). Site-specific ADCs were formulated at 3 mg/mL in PBS pH 7.2. The ADCs were characterized using complementary analytical methods and analytical data are shown in Supplementary Figure S1.

Animals

All studies were conducted at facilities that comply with the principles of the "Guide for Care and Use of Laboratory Animals" and are accredited by the Association for Assessment and Accreditation of Laboratory Animal Care International (AAALAC). All study protocols were approved by the testing facilities Institutional Animal Care and Use Committee. For xenograft efficacy studies, 5- to 6-week-old female athymic (nu/nu) mice were obtained from Harlan Sprague–Dawley Inc. For patient-derived xenograft (PDX) efficacy studies, 6- to 8-week-old female BALB/c nude mice were obtained from Shanghai Sino-British SIPPR/BK Laboratory Animal Co., Ltd. For safety studies, 8- to 12-week-old male Sprague–Dawley rats were obtained from Harlan Laboratories and 2- to 4-year-old male cynomolgus monkeys (Macaca fascicularis) of Cambodian origin were obtained from a commercial supplier.

Mouse efficacy studies

EphA2$^+$ prostate cancer xenograft model: 5×10^6 PC3 (human prostate cancer cell lines) were implanted subcutaneously into the right flank of mice (seven per group). 5T4$^+$ breast cancer xenograft

model: mice were supplemented with 60-day 0.36-mg slow-release estradiol pellets the day before 1×10^7 MDA-MB-361 tumor cells in 50% Matrigel were implanted subcutaneously into the second mammary fat pad (10 per group). $5T4^+$ gastric cancer xenograft model: 5×10^6 N87 cells in 50% Matrigel were injected subcutaneously into the second mammary fat pad of mice (five per group). Target expression was confirmed by immunohistochemistry as previously described (16, 19). Low $5T4^+$ (1^+ by IHC) ST-02-009 gastric PDX model: mice (10 per group) were implanted subcutaneously into right flank with ST-02-009 passage 4 (P4) tumor slices (~30 mm^3). High $5T4^+$ (3^+ by IHC) ST-02-0164 gastric PDX model: mice (10 per group) were implanted subcutaneously into right flank with ST-02-0164 P4 tumor slices (~30 mm^3). When the mean tumor volume was about ~150 to 200 mm^3, tumor-bearing mice were randomized into treatment groups. Test articles were administrated intravenously at indicated dose and dosing frequency (SD, single dose; or FD, fractionated weekly doses × 3). Dose levels for each ADC were chosen based on minimum efficacious dose (MED) determined in single-dose pilot studies. Tumors were measured twice weekly using calipers. Tumor volumes were calculated using the formula 0.5 x L x W^2 (L is the length; W is the width). Animals were euthanized when tumor volumes reached approximately 2,000 mm^3.

Rat safety study

Male Sprague–Dawley rats (six per group) were administered either a single intravenous injection (day 1) of 1.5 mg/kg or three weekly intravenous injections (days 1, 8, and 15) of 0.5 mg/kg anti-EphA2 antibody conjugated to SG3249 (1C1-SG3249). Toxicokinetic (TK) satellite animals (six per group; PK sparse sampling/three samples per timepoint) were included in each treatment arm to measure plasma concentration of total antibody and ADC. Control rats (six per group) were administered a single intravenous injection of vehicle control on day 1. All main study animals were evaluated for clinical signs, changes in body weight, clinical pathology, gross pathology with organ weights, and microscopic observations. All TK satellite animals were evaluated for clinical signs, changes in body weight, and pharmacokinetic analysis.

Hematology and serum chemistry samples were collected and analyzed on days 8 and 15. These timepoints were chosen to evaluate the effects of repeated dosing with 1C1-SG3249 without exceeding blood draw limits for rats. Blood samples for pharmacokinetic analysis were collected from TK satellite animals in K_2 EDTA tubes at multiple time points on days 1, 2, 3, 8, 15, 16, 22, and 29.

A gross necropsy was performed on day 29 on all main study animals and organs, including brain, lung, liver, kidney, spleen, thymus, testes, heart, and bone, were embedded in paraffin, sectioned, stained with hematoxylin and eosin, and examined by light microscopy.

Monkey safety study

Male cynomolgus monkeys (three per group) were administered either a single intravenous injection of 4.5 mg/kg (day 1) or three weekly intravenous injections of 1.5 mg/kg (days 1, 8, and 15) R347 antibody conjugated to SG3400 (R347-SG3400) via the saphenous vein. Because of ethical considerations associated with nonhuman primate (NHP) use, no control animals were assigned to the study and treatment-related effects were assessed by comparing safety endpoints to prestudy values. All animals were evaluated for clinical signs, changes in body weight, clinical pathology, food consumption, ophthalmology assessments, pharmacokinetic analysis, gross pathology with organ weights, and microscopic observations.

Blood samples were collected for clinical pathology via a single draw and divided into K_2 EDTA tubes for hematology, serum separator tubes for serum chemistry, and sodium citrate tubes for coagulation. Hematology and serum chemistry samples were collected and analyzed weekly beginning on day 8 to day 72. Blood samples for pharmacokinetic analysis were collected in K_2 EDTA tubes at multiple time points on days 1, 2, 3, 8, 15, 16, 22, and 36.

A gross necropsy was performed on day 72 on all main study animals and organs, including brain, lung, liver, kidney, spleen, thymus, testes, heart, and bone, were embedded in paraffin, sectioned, stained with hematoxylin and eosin, and examined by light microscopy.

Statistical analysis

Data from safety and efficacy studies are reported as means ± SEM. Statistical analyses comparing means between three or more groups were performed using one-way ANOVA with Newman–Keuls *post hoc* test. All analyses were performed with Prism 6 software (GraphPad Software). Differences were considered significant when #, $P < 0.05$.

Quantitation of 1C1-SG3249 ADC, total antibody, and warhead concentrations in rat plasma

1C1-SG3249 ADC, total antibody, and free warhead (SG3199) in rat K_2EDTA plasma samples were quantitated using LC/MS-MS technology as described previously (17). Briefly, samples were diluted with 0.1% BSA/Tris-Tween buffer and split into two aliquots. Total antibody quantification was performed in SILuMab (Sigma Aldrich) internal standard-spiked samples. Following magnetic Protein A bead capture, a trypsin digest was performed to generate characteristic peptides (VVSVLTVLHQDWLNGK and TTPPVLDSDGSFFLYSK) used as quantitative surrogates of total antibody concentration. For quantitation of ADC, samples were immunoprecipitated with Protein A magnetic beads followed by papain digestion to release warhead. The concentration of the released drug is proportional to the antibody conjugated drug concentration. Deuterium-labeled warhead was used as an internal standard for ADC quantitation. The final extracts for analytes were quantitated using HPLC with triple quadrupole MS/MS detection using positive ion electrospray. A linear, $1/\text{concentration}^2$ weighted regression was used to quantitate unknown samples from the standard curve. The calibration range was 0.05 to 10 μg/mL for total antibody and 0.051 to 10.2 μg/mL for ADC. Dilutional linearity was verified with ultra-high QC samples during assay qualification; any sample with a concentration above the upper limit of the calibration range was diluted 10-fold to obtain results within the established assay limits. Final results, which are reported in neat matrix, are inclusive of the applied dilution. Free warhead was measured by LC/MS-MS as described previously (17) using deuterium-labeled SG3199 as an internal standard. Free warhead/internal standard peak area ratios were utilized for the construction of calibration curves, using weighted ($1/X_2$) linear least-squares regression. The lower limit of quantitation (LLOQ) of free warhead is 0.2 nmol/L.

Quantitation of R347-SG3400 total antibody concentrations in cynomolgus monkey plasma

Total antibody concentrations of R347-SG3400 in cynomolgus monkey K_2EDTA plasma were determined using a qualified universal ELISA method. An ELISA method was chosen for this study after comparability studies demonstrated no significant differences between ELISA and LC/MS methods. Briefly, sheep anti-human IgG (H+L) antibody (The Binding Site) was used to coat Nunc Maxisorp plates up to 72 hours at 2 to 8°C at a concentration of 1 μg/mL in 50 mmol/L carbonate buffer. Following a block step with I-Block buffer, samples (diluted 1/10 in I-Block) were incubated on the blocked plate. The captured R347-SG3400 antibody was detected with goat anti-human IgG (H+L) horseradish peroxidase (HRP, Bethyl Laboratories). Tetramethylbenzidine chromogenic substrate was used to measure the binding complex; once stopped with 2 N H_2SO_4, the plate was read at 450 and 650 nm, and the intensity of color development was directly proportional to levels of total antibody in sample. Dilutional linearity was verified with ultra-high QC samples during assay qualification. Sample results were reported in ng/mL; the lower limit of quantitation was 50 ng/mL. Total ADC and free warhead were not assessed in this study as previous *in vivo* studies confirmed that our site specific PBDs are highly stable with limited deconjugation (17). As a result, total antibody can be used as a reliable surrogate for ADC exposure.

Pharmacokinetic analysis

A standard noncompartmental analysis (NCA) for a bolus intravenous administration was used for all pharmacokinetic data analysis using Phoenix 64 WinNonlin 6.3 (Pharsight). The maximum observed peak plasma concentration (C_{max}), area under the plasma concentration versus time curve (AUC) and half-life ($t_{1/2}$) of elimination phase were estimated and summarized statistically as mean and 1 SD. Rat $AUC_{0\text{-}28}$ was calculated using NCA and compared to $AUC_{0\text{-}28}$ calculated using population PK analysis to verify NCA did not overestimate the exposure (AUC) in rats. Because the two values were similar, only NCA-estimated rat $AUC_{0\text{-}28}$ is reported in the results. Because of limited monkey PK time points, monkey PK data was modeled using a two-compartment population PK model with linear elimination (NONMEM 7.2) and model-based population predictions (PRED) were used to monkey calculate $AUC_{0\text{-}28}$.

Results

Tumor regression in mice is comparable following single or fractionated dose regimens of tumor-targeting PBD ADCs

Mouse xenograft and PDX models of human cancer were used to compare the antitumor activity of PBD ADCs after single and fractionated dosing (Fig. 1). Preliminary studies were conducted in cell-line-derived xenograft models of $EphA2^+$ human prostate cancer (Fig. 1A), as well as $5T4^+$ human gastric (Fig. 1B) and breast (Fig. 1C) cancer, to evaluate the exposure-activity across target antigens and tumor types. Results were similar across models, with both dosing schedules resulting in significant antitumor activity that persisted until day 61 of study. In the human prostate cancer model, mice were treated with anti-EphA2 PBD ADC (1C1-SG3249) or negative control R347 PBD ADC (R347-SG3249) administered as either an SD of 1.5 mg/kg or as three weekly fractionated doses of 0.5 mg/kg (Fig. 1A). Although both dosing schedules were equally effective over the long term, the time-to-tumor regression was slightly slower in mice treated with three weekly doses compared to mice treated with an SD of 1C1-SG3249 (day 43 vs. day 32, respectively). As expected, limited antitumor activity was observed in mice treated with negative control R347-SG3249. In the human gastric and breast cancer xenograft models, mice were treated with an anti-5T4 PBD ADC (5T4-SG3249) as an SD of 1 mg/kg or as three weekly fractionated doses of 0.33 mg/kg (Fig. 1B and C). As with the PC3 prostate model, single and fractionated dosing schedules were equally effective over the study period, although the time-to-tumor regression was again slightly faster after single-dose treatment in both models. The impact of dosing regimen on antitumor activity was further evaluated by comparing single and fractionated dosing schedules of 5T4-SG3249 in two gastric PDX models with variable 5T4 expression (Fig. 1D and E). As in xenograft models, fractionated dosing resulted in comparable antitumor activity with longer time-to-tumor regression in the low 5T4-expressing tumor model (Fig. 1D). In contrast, no differences in antitumor activity were observed in the high 5T4-expressing tumor after single or fractionated dosing (Fig. 1E). Moreover, tumor regrowth was significantly delayed in mice treated with fractionated dosing. Although there is a trend toward slightly delayed onset of antitumor activity after fractionated dosing, overall, the data indicate that single and fractionated dosing schedules of targeted PBD ADCs have comparable antitumor activity in human cancer mouse models.

Fractionated dosing improved the tolerability of 1C1-SG3249 in rats

Next, we evaluated whether fractionated dosing affected the tolerability of 1C1-SG3249 in a rat toxicity study (Fig. 2A–F). For this, we compared body weight gain—a primary toxicology endpoint used to assess overall health of animals (23)—across three groups of rats (six per group) treated with vehicle control, an SD of 1.5 mg/kg 1C1-SG3249 or three weekly fractionated doses of 0.5 mg/kg 1C1-SG3249. Treatment with an SD of 1.5 mg/kg SG3249 had the greatest impact on body weight gain relative to vehicle control rats (Fig. 2B). Animals administered an SD of 1.5 mg/kg experienced a significant reduction (~10%; $P < 0.05$ vs. control) in body weight gain starting on day 8. These effects became increasing severe over time (up to ~20% on day 11; $P < 0.001$ vs. control) and persisted until the end of study. A significant reduction in body weight gain was also detected in rats treated with fractionated dosing; however, the effects were generally milder and delayed in onset compared to single-dose treatment. From day 11 onward, a small decrease in body weight gain (~3%; $P < 0.05$ vs. control) was observed that continued to decline (up to ~10% $P < 0.001$ vs. control) until the end of study. Myelotoxicity was the primary dose-limiting toxicity observed in rats (Fig. 2C–F). Hematologic analysis on days 8 and 15 demonstrated that treatment with an SD of 1.5 mg/kg 1C1-SG3249 resulted in significant decreases in several hematologic parameters, including hematocrit, neutrophils, white blood cells, and reticulocytes. The severe neutropenia (<0.5 cells • 10^3/μL) observed on days 8 and 15 was likely a significant factor contributing to early mortality secondary to infection in these animals (Fig. 2C). In contrast, fractionated dosing was associated with less severe

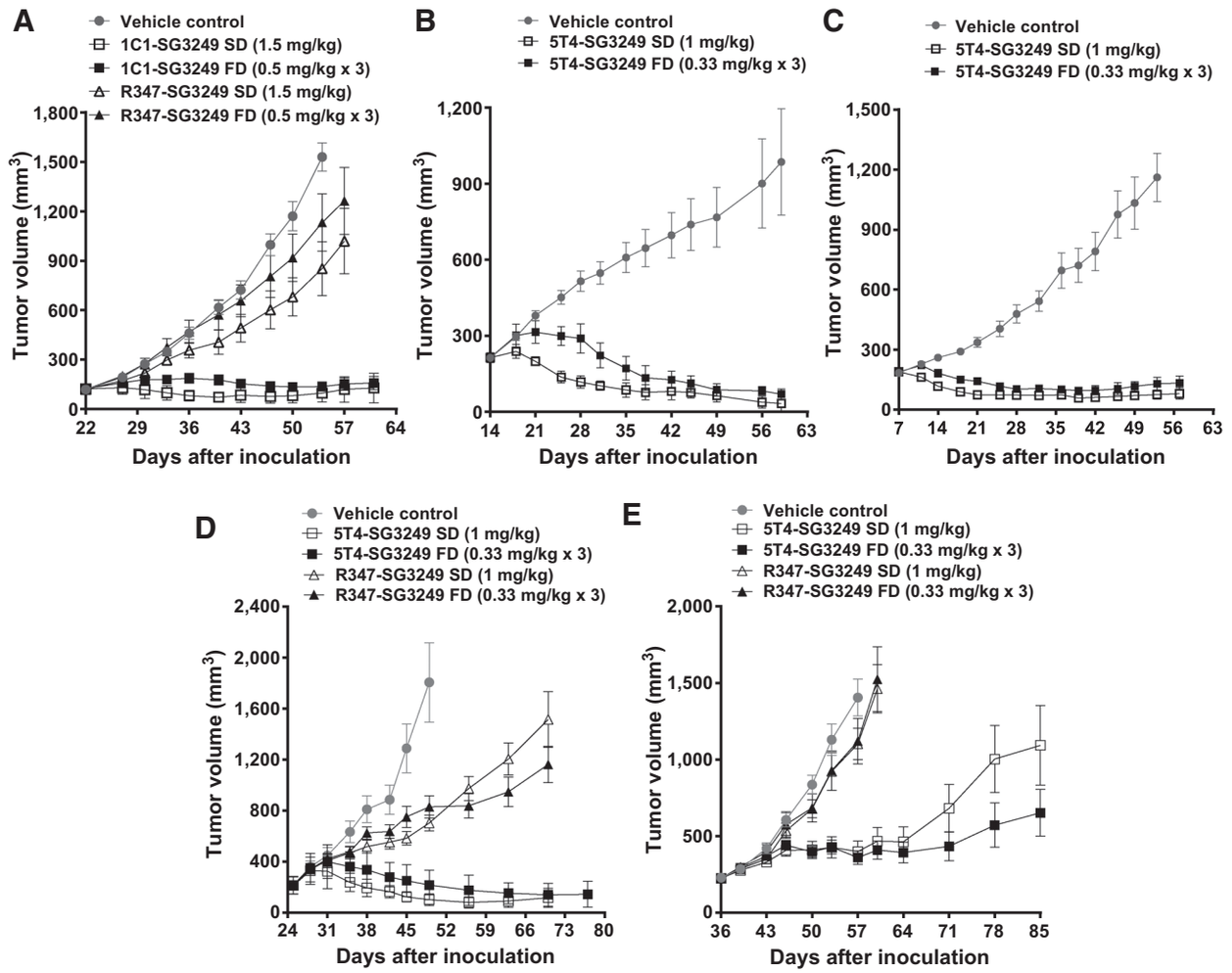

Figure 1.

Comparable antitumor activity after single or fractionated dosing with PBD ADCs in preclinical mouse tumor models. **A–E,** Single (SD) and fractionated (FD) dosing schedules were evaluated in (**A**) an EphA2$^+$ human prostate cancer cell line (PC3) xenograft model, (**B**) a 5T4$^+$ human gastric cancer N87 xenograft model, (**C**) a 5T4$^+$ human breast cancer MDA-MB-361 xenograft model, and (**D, E**) two PDX gastric cancer models with (**D**) low 5T4 expression or (**E**) high, heterogeneous 5T4 expression, as determined by immunohistochemistry. When the mean tumor volume reached 150 to 200 mm^2, female athymic (nu/nu) mice (5–10/group) were treated with an SD or FD doses of vehicle control or a tumor-targeting PBD ADC [(**A**) 1C1-SG3249, (**B–E**) 5T4-SG3249] by intravenous injection. Where indicated (**A, D, E**), animals were similarly treated with an isotype-matched PBD ADC (R347-SG3249) to serve as a negative control group. Results are represented as the mean ± SEM of each group at individual timepoints.

myelosuppression as noted by less impact on the same hematologic parameters. In the case of neutrophils, although there was some decrease compared to controls, mean absolute cells counts remained within normal range for male rats (0.84–2.67 cells • $10^3/\mu L$; ref. 24) at both timepoints. In addition, no signs of cumulative bone marrow toxicity were observed after repeated dosing on day 15 compared to day 8. Histopathologic analysis of bone marrow was performed; however, a direct comparison of fractionated and single-dose regimens was not possible as all animals were necropsied on day 29, after extensive recovery had occurred.

Although fractionated dosing improved overall survival and myelotoxicity in rats, it did not appear to impact ocular toxicity associated with 1C1-SG3249 treatment. Histopathology analysis indicated that both dosing regimens were associated with mild to moderate macroscopic observations of bilateral corneal opacity corresponding with acute inflammation of the anterior segment (Supplementary Table S1). This finding was unexpected as ocular toxicity has not been reported as an adverse event of PBD ADCs in animals and was not observed in rats treated with isotype control R347-SG3249 in a pilot single-dose toxicity study (Supplementary Table S1). It is possible that this finding could be related to normal tissue expression as EphA2 expression has been reported in corneal epithelial cells (25) and loss of EphA2 receptor function has been associated with cataract development (26). Although it is unclear why fractionated dosing improved some organ-specific toxicities and not others, it is possible that dosing schedule might not have as great an influence on target-dependent toxicities due to receptor-mediated uptake (27).

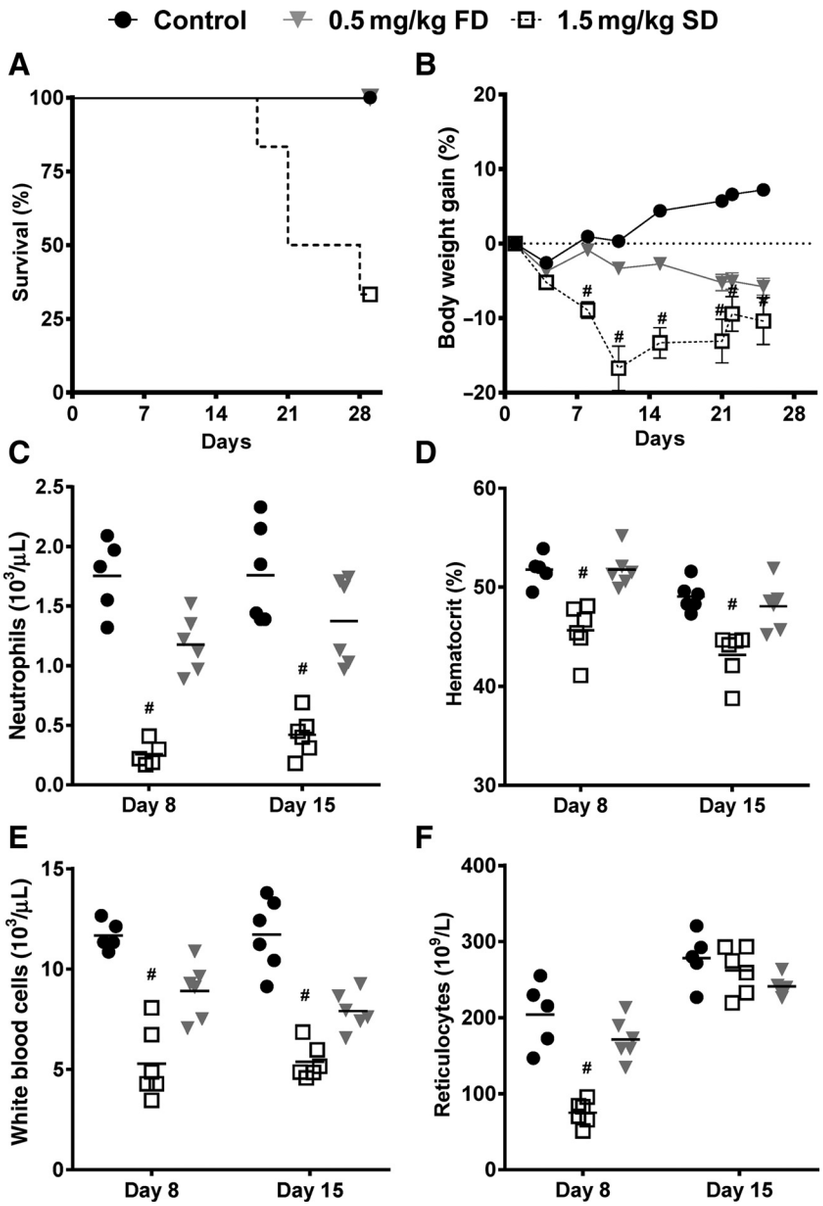

Figure 2.

Fractionated dosing improves tolerability of PBD ADC in rats. Rats ($n = 6$) were treated with a single intravenous injection (1.5 mg/kg SD) or three weekly fractionated intravenous injections (0.5 mg/kg FD) of an anti-EphA2 PBD ADC (1C1-SG3249). Control animals were treated with a single intravenous injection of vehicle control. **A** and **B,** Tolerability was assessed by measuring percent (**A**) survival and (**B**) body weight gain in rats over a 29-day period. A total of four animals treated with an SD of 1.5 mg/kg 1C1-SG3249 were euthanized due to moribund condition or found dead between days 18 and 29 of study. Data points represent the mean value of each group at individual timepoints; error bars, mean ± SEM. **C–F,** Improved tolerability of fractionated dosing associated with reduced impact on peripheral blood cell counts. Hematologic analysis was conducted on peripheral blood samples collected on days 8 and 15. Bars represent the mean value of each group; error bars, mean ± SEM. #, $P < 0.05$ versus SD-treated rats.

Fractionated dosing also improves tolerability of a structurally related PBD ADC in monkeys

A follow up toxicology study was conducted in cynomolgus monkeys to assess applicability of these findings across species. We chose monkeys for this study as they are the most commonly used toxicology species to evaluate the safety of biopharmaceutical products (28); however, due to ethical considerations associated with use of NHP, we were limited in the number of ADC constructs we could evaluate. Therefore, the study was designed to evaluate whether the findings observed with SG3249-based ADC could be applied to other PBD ADCs while using the minimum number of animals. SG3400 was chosen as the payload as it is structurally similar to SG3249; however, the *in vitro* potency of the warhead component (SG2000; ref. 22) is approximately 10-fold less potent than the warhead component of SG3249 (SG3199; refs. 20, 21). R347, an IgG1 isotype control antibody (29), was chosen for the antibody component in order to eliminate potential confounding factors related to target expression. This construct was then used to test whether fractionated dosing improves tolerability of a structurally related PBD ADC. Male monkeys (three per group) were treated with an SD of 4.5 mg/kg or three weekly fractionated doses of 1.5 mg/kg of R347 antibody conjugated to SG3400 (R347-SG3400) by intravenous injection. No control animals were included in the study to further minimize use of NHP; therefore, treatment-related findings were assessed by comparing safety endpoints to prestudy values.

All monkeys survived to the end of study after single or fractionating dosing with R347-SG3400. However, monkeys treated with an SD exhibited a notable decline in body weight on day 8 that peaked on day 36 and remained below prestudy values throughout the study period (Fig. 3A). In comparison, despite

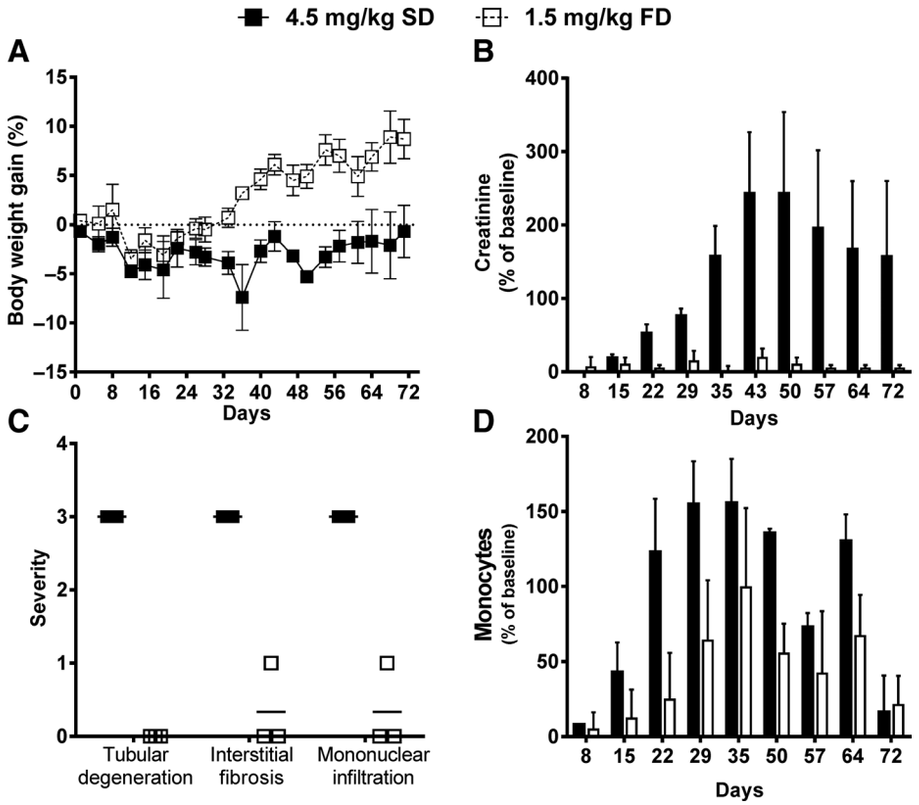

Figure 3.

Similar improvements in tolerability after fractionated dosing of a structurally related PBD ADC in monkeys. Male monkeys ($n = 3$) were treated with a single IV injection (4.5 mg/kg SD) or three weekly fractionated intravenous injections (1.5 mg/kg FD) of a nontargeted PBD ADC (R347-SG3400). No control animals were included due to ethical considerations related to use of nonhuman primates. As a result, treatment-related findings were assessed by comparing all values to baseline. **A,** Tolerability was assessed by measuring percent (**A**) body weight gain in monkeys over a 72-day period. Data points represent the mean value of each group at individual timepoints; error bars, mean ± SEM. **B–D,** Improved tolerability of fractionated dosing associated with decreased kidney injury as assessed by (**B**) decreased serum creatinine, a biomarker of renal injury, (**C**) decreased histopathologic observations of tubular degeneration, interstitial fibrosis, and mononuclear infiltration, and (**D**) reduced monocytosis. Bars represent the mean value of each group; error bars, mean ± SEM. Histopathology severity classified as 1 = slight, 2 = mild, 3 = moderate, 4 = severity.

an early transient drop in body weight, monkeys treated with a fractionated dosing schedule exhibited marked body weight gain over the course of the study. Clinical signs of discolored skin (black, red), alopecia, squinting of the eyes, and nasal discharge were observed in the animals that received an SD of 4.5 mg/kg of R347-SG3400. Although similar clinical signs were observed in the fractionated dosing group, the findings were less severe and/or limited in duration. Together, these results suggest fractionated dosing also improved tolerability of a structurally related, but chemically distinct, PBD ADC in monkeys.

Fractionated dosing also appeared to improve kidney injury associated with R347-SG3400 treatment (Fig. 3B and C). Monkeys treated with an SD of 4.5 mg/kg exhibited a delayed increase in serum creatinine, a biomarker of kidney injury, on day 22 (FIG. 3B). Serum creatinine levels continued to increase with time, peaking on day 50 (up to 3 mg/dL), and remaining elevated until the end of the study. In contrast, serum creatinine in monkeys treated with fractionated dosing remained near baseline until day 72. Histopathologic analysis confirmed that elevations in serum creatinine were associated with kidney injury characterized by moderate interstitial fibrosis with mononuclear cell infiltration, moderate tubular atrophy, and moderate tubular degeneration/regeneration in all animals treated with an SD of R347-SG3400 (Fig. 3C). By comparison, the severity of these findings was greatly reduced to mild, or not present, in monkeys treated with a fractionated dosing schedule. Treatment with an SD was also associated with significant monocytosis (>1×10^3 cells/mL; ref. 30), likely secondary to kidney injury, on day 15 that persisted until day 64 (Fig. 3D). In contrast, monocytes counts in monkeys treated with fractionated dosing were significantly lower and did not exceed 1×10^3/mL at any timepoint.

Comparable total exposure after single or fractionated dosing with PBD ADCs in rats and monkeys

Plasma concentrations of intact ADC, total antibody (conjugated and unconjugated 1C1 antibody), and free SG3199 warhead were measured in rats (Fig. 4). Following intravenous administration of an SD of 1.5 mg/kg or 3 weekly fractionated doses of 0.5 mg/kg, 1C1 ADC exhibited linear PK. The area under concentration–time curve from time 0-to-7 days post-dose ($AUC_{0\text{-}7}$) increased dose proportionally from 30.3 μg*day/mL at 0.5 mg/kg to 85.2 μg*day/mL at 1.5 mg/kg (Supplementary Table S2). Furthermore, total plasma exposure over 28-day study period ($AUC_{0\text{-}28}$) was comparable following the SD of 1.5 mg/kg (125.3 μg*day) and 3 weekly fractionated doses of 0.5 mg/kg (129.9 μg*day/mL). As expected, peak plasma concentration (36.8 μg/mL) after an SD of 1.5 mg/kg was approximately three-fold higher than that (11.5 μg/mL) of the fractionated dose group. The high C_{max} in the single-dose group appeared to inversely correspond to the low tolerability, suggesting a C_{max} associated tolerability in rats. Free warhead levels remained below the limit of detection (0.2 nmol/L) at all timepoints. This, in addition to the comparable pharmacokinetic profile of intact ADC and total antibody, indicated limited deconjugation of SG3249 from the ADC.

Similarly, plasma exposure ($AUC_{0\text{-}7}$) of total antibody following intravenous administration of R347-SG3400 ADC in cynomolgus monkeys increased approximately dose-proportionally from

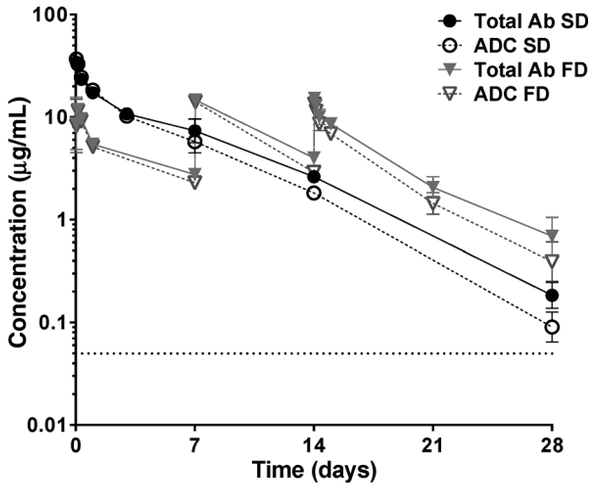

Figure 4.

Comparable exposure in rats treated with single versus fractionated dosing regimens of PBD ADC. Plots of mean concentration vs time of total of total antibody (solid line) and ADCs (dashed line) in rats (six per group) treated with an SD of 1.5 mg/kg or three weekly (FD) of 0.5 mg/kg 1C1-SG3249 by intravenous injection. Each time point is the mean values ± SD of three sparse samples. The dashed line represents the LLOQ, which was 0.05 μg/mL for both total antibody and ADC.

80.7 μg*day/mL at 1.5 mg/kg to 261.4 μg*day/mL at 4.5 mg/kg, indicating linear PK in monkeys (Table 1). Peak plasma concentration of total antibody was about threefold higher or dose-proportionally in the single high dose of 4.5 mg/kg group (102.0 μg/mL) than in the low dose of 1.5 mg/kg (31.1 μg/mL), which is consistent with reduced tolerability in this group. A population PK model was used to fit observed PK data, and $AUC_{0\text{-}28}$ was thus calculated based on population prediction (PRED) of the population PK model (Supplementary Fig. S2 and Table 1). Using this model, it is predicted that $AUC_{0\text{-}28}$ should be comparable after single (581.9 μg*day/mL) or fractionated dosing (526 μg*day/mL). Collectively, PK and safety data across species of rat and monkey implicate C_{max}-driven tolerability for PBD ADCs.

Discussion

Despite the highly targeted nature of ADCs, clinical development of these molecules continues to be limited by narrow therapeutic indexes (2, 3). Having a better understanding of the relationship between exposure and toxicity could play a vital role in early clinical trial design by enabling rational selection of dosing schedules. Our studies investigated whether preclinical studies could be used to understand the pharmacokinetic parameters driving efficacy and toxicity in preclinical models. We used dose-fractionation studies to evaluate the impact of lowering peak drug concentrations while maintaining equivalent total exposure. By doing so, we demonstrated that fractionated dosing improved tolerability of highly potent PBD ADCs while maintaining antitumor activity in a preclinical setting.

Because clinical utility is a balance of safety and efficacy, the schedule-dependence of both parameters was evaluated in preclinical models. Although we did not conduct pharmacokinetic analysis in our mouse studies, we anticipate that total exposure or AUC would be similar in mice treated with single or fractionated dosing as ADC PK in tumor-bearing mice is linear and similar to that in nontumor-bearing mice (17, 31). Therefore, on the efficacy side, preliminary data from mouse xenograft and PDX models suggests that antitumor activity of at least some PBD ADC is more closely correlated to total exposure than C_{max} (Figs. 1 and 4). However, given that this is based on data from a small number of models, it is unknown how broadly these findings will translate across tumor targets and histologies. To our knowledge, there have been no publications exploring the impact of dosing schedule on preclinical efficacy with PBD ADCs, indicating that additional work is needed to understand the broad applicability of these results. However, given the low tumor penetration and limited tissue distribution of antibodies (32), high peak plasma concentrations are not anticipated to increase antitumor activity of an ADC (33). Moreover, similar findings have been observed with other classes of ADCs, such as those conjugated to microtubule-inhibiting payloads. Data from a recent publication by Govindan and colleagues (34), demonstrated that antitumor activity of T-DM1, a HER2-targeting ADC conjugated to the maytansinoid DM1, was similar in animals treated with single or fractionated dosing schedules. In addition, dose fractionation studies with IMMU-130, a CEACAM5-targeting ADC conjugated to the DNA topisomerase I inhibitor, 7-ethyl-10-hydroxycamptothecin (SN-38), have also shown comparable antitumor activity with single and fractionated dosing regimens (35). Taken together, these data suggest preclinical anti-tumor activity of ADCs could be more closely associated with total exposure rather than the peak concentration.

On the safety side, preliminary data from rat and monkey toxicology studies suggest that dosing schedule can also significantly impact preclinical tolerability of PBD ADCs. Fractionated dosing was associated with a significant improvement in body weight changes in both species. Pharmacokinetic analysis in rats and monkeys revealed that C_{max}, but not AUC, appeared to correlate with preclinical tolerability, suggesting that tolerability of ADCs may be more closely associated with C_{max} then total exposure. Organ-specific toxicities were also affected by dosing schedule. In rats, where bone marrow suppression is a major dose-limiting toxicity of PBD ADCs (36), fractionated dosing showed significantly less effects of 1C1-SG3249 on peripheral blood counts compared to the single-dose group. In monkeys,

Table 1. Pharmacokinetics of R347-SG3400 after single or fractionated dosing in monkeys (three/group)

Treatment	Analyte	[a]C_{max} (μg/mL)	$t_{1/2}$ (day)	$AUC_{0\text{–}7}$ (day* μg/mL)	$AUC_{0\text{–}28}$ (day* μg/mL)
4.5 mg/kg SD	Total Ab	102.0 (11.2)	10.4 (0.8)	261.4 (37.6)	581.9[b]
1.5 mg/kg FD	Total Ab	31.1 (4.2)		80.7 (8.6)	526.1[b]

PK parameters presented as mean ± (SD).

[a]C_{max} after first dose.

[b]$AUC_{0\text{-}28}$ calculation was based on population predictions (PRED) of PK model.

fractionated dosing with a structurally related ADC also improved organ-specific toxicities—thus confirming that this finding is not restricted to a particular PBD or to a single species. For this study, we used a nontargeted PBD ADC (R347-SG3400) to eliminate the potential for confounding data related to target expression on normal tissues. Unlike SG3249, the major toxicity of R347-SG3400 in monkeys was renal injury. This difference, although not predictable, was not entirely unexpected as the safety profile of cytotoxic agents can be species-specific and/or related to modifications in chemical structure (37). The ability of fractionated dosing to reduce kidney toxicity of an SG3400 ADC was remarkable. A SD of R347-SG3400 resulted in delayed kidney injury that was completely absent in animals treated with a fractionated dosing regimen. This suggests that peak plasma concentration is a major factor driving tubular degeneration in the kidneys of animals treated with PBD ADCs. Together, these data indicate that fractionated dosing can have an overall positive effect on both tolerability and organ-specific toxicities across species with different PBD ADCs.

In addition, the translatability of these findings to patients is not known given the uncertain predictive value of animal models (38). Xenograft mouse models, in particular, are generally not considered reliable predictors of clinical activity due to the significant differences between mouse and human tumor growth characteristics and metastatic behavior. Translatability of preclinical activity of conjugated antibodies is further complicated by significant differences in target distribution and pharmacokinetic profiles across species (39). Despite these uncertainties, confidence in preclinical outcomes can be greatly increased by using a panel of cell line and/or PDX models for each tumor type (40). In our case, we demonstrated that fractionated dosing did not impact antitumor activity of two targeted PBD ADCs across multiple tumor types. Therefore, we believe that these findings should be further explored in other tumor models and ultimately in patients.

Similar to efficacy models, toxicology studies in healthy animals are not always predictive of the dose-limiting toxicities in patients (41). Although there are many variables that impact the clinical predictive value of toxicology studies, one of the major determinants is the organ system involved. In the case of cytotoxic agents—where bone marrow suppression is a common toxicity clearly related to the mechanism of action (42)—animal models are generally predictive of hematologic toxicity in patients (43). Therefore, it seems probable that the benefits of fractionated dosing on bone marrow suppression observed in our study could translate to patients. If so, this finding could be important to clinical trial design of PBD-based ADCs, where bone marrow suppression has been reported as a significant dose-limiting toxicity humans (14, 36, 44). However, toxicology studies are generally less reliable predictors of kidney toxicity, with reports that monkeys, in particular, grossly over predict the incidence of renal injury in humans (43). Therefore, it is possible that the benefits of fractionated dosing on kidney injury might not translate to patients—especially given that renal toxicity has not been a major adverse effect of PBD ADCs in the clinic (14, 44). Despite the difficulties associated with use of preclinical models to understand exposure-response relationships, it is still much easier than trying to identify the pharmacokinetic drivers of safety and efficacy in patients—where clinical pharmacokinetic data are largely derived from a single-dose schedule (45) and most patients have concurrent medical conditions and/or medications that make it complicated to extract a single simple pharmacokinetic parameter directly from clinical safety findings (45).

Another issue that remains to be addressed is whether dose fractionation can improve both on and off target toxicities. Given the limited number of constructs that we could analyze in this study we cannot rule out that dose fractionation might not improve all toxicities, in particular on-target toxicities. While the effect of target expression on exposure–toxicity relationships should be further explored, it is likely a very complex issue given on-target toxicity is not driven solely by target expression and that other factors (e.g., proliferative/regenerative potential of target cell/organ, mechanism/potency of warhead, and accessibility of the ADC to the target cell) could play a role (46). Therefore, at present, the impact of dose-fractionation on the preclinical TI of PBD ADCs should be empirically tested for novel ADCs with different patterns of normal tissue target expression.

In conclusion, these data indicate preclinical dose-fractionation studies could be an important strategy to inform selection of clinical dosing schedule by increasing our understanding of the underlying pharmacokinetic drivers of safety and efficacy for PBD ADCs. While additional work is needed to understand the broad applicability of these data, our work suggests that fractionated dosing could be an important mitigation strategy to widen the therapeutic index of highly potent ADCs in patients.

Disclosure of Potential Conflicts of Interest

A. Tiberghien has ownership interest in AstraZeneca. No potential conflicts of interest were disclosed by the other authors.

Authors' Contributions

Conception and design: B. Zheng, X.Q. Yu, H. Zhong, J. Harper, M. Rebelatto, P.W. Howard, R. Dixit

Development of methodology: B. Zheng, J. Harper, M. Rebelatto, P.W. Howard

Acquisition of data (provided animals, acquired and managed patients, provided facilities, etc.): M.J.M. Hinrichs, S. Breen, C. Chen

Analysis and interpretation of data (e.g., statistical analysis, biostatistics, computational analysis): P.M. Ryan, B. Zheng, X.Q. Yu, M. Gunsior, H. Zhong, J. Harper, K. Vashisht, M. Rebelatto, C. Chen

Writing, review, and/or revision of the manuscript: M.J.M. Hinrichs, P.M. Ryan, S. Afif-Rider, X.Q. Yu, M. Gunsior, H. Zhong, K. Vashisht, M. Rebelatto, P.C. Ryan, C. Chen, P.W. Howard, R. Dixit

Administrative, technical, or material support (i.e., reporting or organizing data, constructing databases): M.J.M. Hinrichs, P.M. Ryan, B. Bezabeh, M. Reed, C. Chen

Study supervision: S. Afif-Rider, H. Zhong, M. Reed, R. Dixit

Other (manufacture, purification and analysis of pyrrolobenzodiazepine-containing antibody drug conjugates for this study): N. Patel

Other (synthesis of materials): L. Masterson

Other (SG3249 synthesis): A. Tiberghien

Other (design of SG3400 and supply of material for study): P.W. Howard

Other (provided antibodies, antibody drug conjugates and related supporting information): N. Dimasi

Acknowledgments

We thank Moucun Yuan, Elizabeth Dompkowski, Michael Waldron, and William Mylott Jr of PPD Laboratories (Richmond, VA) for carrying out LC-MS/MS studies.

The costs of publication of this article were defrayed in part by the payment of page charges. This article must therefore be hereby marked *advertisement* in accordance with 18 U.S.C. Section 1734 solely to indicate this fact.

Received January 25, 2017; revised April 5, 2017; accepted June 13, 2017; published OnlineFirst June 19, 2017.

References

1. Mullard A. Maturing antibody-drug conjugate pipeline hits 30. Nat Rev Drug Discov 2013;12:329–32.
2. Sassoon I, Blanc V. Antibody–drug conjugate (ADC) clinical pipeline: a review. In:Ducry L, editor.Antibody-drug conjugates. Totowa, NJ: Humana Press; 2013. p. 1–27.
3. Donaghy H.Effects of antibody, drug and linker on the preclinical and clinical toxicities of antibody-drug conjugates. mAbs 2016;8:659–71.
4. Castaigne S, Pautas C, Terre C, Raffoux E, Bordessoule D, Bastie JN, et al. Effect of gemtuzumab ozogamicin on survival of adult patients with de-novo acute myeloid leukaemia (ALFA-0701): a randomised, open-label, phase 3 study. Lancet 2012;379:1508–16.
5. Deslandes A.Comparative clinical pharmacokinetics of antibody-drug conjugates in first-in-human Phase 1 studies. mAbs 2014;6:859–70.
6. Beeram M, Krop IE, Burris HA, Girish SR, Yu W, Lu MW, et al. A phase 1 study of weekly dosing of trastuzumab emtansine (T-DM1) in patients with advanced human epidermal growth factor 2-positive breast cancer. Cancer 2012;118:5733–40.
7. Fanale MA, Forero-Torres A, Rosenblatt JD, Advani RH, Franklin AR, Kennedy DA, et al. A phase I weekly dosing study of brentuximab vedotin in patients with relapsed/refractory CD30-positive hematologic malignancies. Clin Cancer Res 2012;18:248–55.
8. Younes A, Kim S, Romaguera J, Copeland A, Farial Sde C, Kwak LW, et al. Phase I multidose-escalation study of the anti-CD19 maytansinoid immunoconjugate SAR3419 administered by intravenous infusion every 3 weeks to patients with relapsed/refractory B-cell lymphoma. J Clin Oncol 2012;30:2776–82.
9. Ribrag V, Dupuis J, Tilly H, Morschhauser F, Laine F, Houot R, et al. A dose-escalation study of SAR3419, an anti-CD19 antibody maytansinoid conjugate, administered by intravenous infusion once weekly in patients with relapsed/refractory B-cell non-Hodgkin lymphoma. Clin Cancer Res 2014; 20:213–20.
10. Taksin AL, Legrand O, Raffoux E, de Revel T, Thomas X, Contentin N, et al. High efficacy and safety profile of fractionated doses of Mylotarg as induction therapy in patients with relapsed acute myeloblastic leukemia: a prospective study of the alfa group. Leukemia 2006;21:66–71.
11. Peterlin P, Guillaume T, Delaunay J, Mohty M, Garnier A, Mahe B, et al. Similarity of fractionated versus single dose(s) of gemtuzumab ozogamicin as part of the MIDAM salvage regimen in relapsed/refractory acute myeloid leukemia patients. Sem Hematol 2016;53:216–7.
12. Peterlin P, Guillaume T, Delaunay J, Mohty M, Garnier A, Rialland F, et al. No advantages of fractionated versus single dose(s) of gemtuzumab ozogamicin (GO) as part of the midam salvage regimen in relapsed/refractory acute myeloid leukemia (AML) patients. Blood 2015;126:2520.
13. Wilkinson GP, Taylor JP, Shnyder S, Cooper P, Howard PW, Thurston DE, et al. Preliminary pharmacokinetic and bioanalytical studies of SJG-136 (NSC 694501), a sequence-selective pyrrolobenzodiazepine dimer DNA-cross-linking agent. Invest New Drugs 2004;22:231–40.
14. Rudin CM, Pietanza MC, Bauer TM, Spigel DR, Ready N, Morgensztern D, et al. Safety and efficacy of single-agent rovalpituzumab tesirine (SC16LD6.5), a delta-like protein 3 (DLL3)-targeted antibody-drug conjugate (ADC) in recurrent or refractory small cell lung cancer (SCLC). J Clin Oncol 2016;34(Suppl/abstr LBA8505).
15. Stein AS, Walter RB, Erba HP, Fathi AT, Advani AS, Lancet JE, et al. A phase 1 trial of SGN-CD33A as monotherapy in patients with CD33-positive acute myeloid leukemia (AML). Blood 2015;126:324.
16. Jackson D, Gooya J, Mao S, Kinneer K, Xu L, Camara M, et al. A human antibody-drug conjugate targeting EphA2 inhibits tumor growth in vivo. Cancer Res 2008;68:9367–74.
17. Thompson P, Fleming R, Bezabeh B, Huang F, Mao S, Chen C, et al. Rational design, biophysical and biological characterization of site-specific antibody-tubulysin conjugates with improved stability, efficacy and pharmacokinetics. J Controlled Rel 2016;236:100–16.
18. Dimasi N, Fleming R, Zhong H, Bezabeh B, Kinneer K, Christie RJ, et al. Efficient preparation of site-specific antibody–drug conjugates using cysteine insertion. Mol Pharm 2017;14:1501–16.
19. Sapra P, Damelin M, DiJoseph J, Marquette K, Geles KG, Golas J, et al. Long-term tumor regression induced by an antibody–drug conjugate that targets 5T4, an oncofetal antigen expressed on tumor-initiating cells. Mol Cancer Therap 2013;12:38–47.
20. Tiberghien AC, Levy J-N, Masterson LA, Patel NV, Adams LR, Corbett S, et al. Design and synthesis of tesirine, a clinical antibody–drug conjugate pyrrolobenzodiazepine dimer payload. ACS Med Chem Lett 2016;7:983–87.
21. Hartley JA, Spanswick VJ, Brooks N, Clingen PH, McHugh PJ, Hochhauser D, et al. SJG-136 (NSC 694501), a novel rationally designed DNA minor groove interstrand cross-linking agent with potent and broad spectrum antitumor activity. Part 1: Cellular pharmacology, in vitro and initial in vivo antitumor activity. Cancer Res 2004;64: 6693–9.
22. Rahman KM, Thompson AS, James CH, Narayanaswamy M, Thurston DE. The pyrrolobenzodiazepine dimer SJG-136 forms sequence-dependent intrastrand DNA cross-links and monoalkylated adducts in addition to interstrand cross-links. J Am Chem Soc 2009;131:13756–66.
23. Ullman-Cullere MH, Foltz CJ. Body condition scoring: a rapid and accurate method for assessing health status in mice. Lab Anim Sci 1999;49:319–23.
24. Clinical Laboratory Parameters for Crl:CD(SD) Rats [Internet]. Charles River Laboratories. 2006 [cited 2016]. Available from:http://www.criver.com/files/pdfs/rms/cd/rm_rm_r_clinical_parameters_cd_rat_06.aspx.
25. Kaplan N, Fatima A, Peng H, Bryar PJ, Lavker RM, Getsios S. EphA2/Ephrin-A1 signaling complexes restrict corneal epithelial cell migration. Invest Ophthal Visual Sci 2012;53:936–45.
26. Dave A, Martin S, Kumar R, Craig JE, Burdon KP, Sharma S. Epha2 mutations contribute to congenital cataract through diverse mechanisms. Mol Vision 2016;22:18–30.
27. Mager DE.Target-mediated drug disposition and dynamics. Biochem Pharmacol 2006;72:1–10.
28. Preclinical safety evaluation of biotechnology-derived pharmaceuticals ICH harmonized tripartite guideline S6(R1), 2011. Available at http://www.ich.org/fileadmin/Public_Web_Site/ICH_Products/Guidelines/Safety/S6_R1/Step4/S6_R1_Guideline.pdf.
29. Bachelder RE, Bilancieri J, Lin W, Letvin NL. A human recombinant Fab identifies a human immunodeficiency virus type 1-induced conformational change in cell surface-expressed CD4. J Virol 1995;69: 5734–42.
30. Park H-K, Cho J-W, Lee B-S, Park H, Han J-S, Yang M-J, et al. Reference values of clinical pathology parameters in cynomolgus monkeys (Macaca fascicularis) used in preclinical studies. Lab Animal Res 2016;32:79–86.
31. Leal M, Wentland J, Han X, Zhang Y, Rago B, Duriga N, et al. Preclinical Development of an anti-5T4 antibody-drug conjugate: pharmacokinetics in mice, rats, and NHP and tumor/tissue distribution in mice. Bioconjug Chem 2015;26:2223–32.
32. Lee CM, Tannock IF. The distribution of the therapeutic monoclonal antibodies cetuximab and trastuzumab within solid tumors. BMC Cancer 2010;10:255–66.
33. Levison ME, Levison JH. Pharmacokinetics and pharmacodynamics of antibacterial agents. Infect Dis Clin North America 2009;23:791–815, vii.
34. Jumbe NL, Xin Y, Leipold DD, Crocker L, Dugger D, Mai E, et al. Modeling the efficacy of trastuzumab-DM1, an antibody drug conjugate, in mice. J Pharmacokinetics Pharmacodynamics 2010;37:221–42.
35. Govindan SV, Cardillo TM, Rossi EA, Trisal P, McBride WJ, Sharkey RM, et al. Improving the therapeutic index in cancer therapy by using antibody–drug conjugates designed with a moderately cytotoxic drug. Mol Pharm 2015;12:1836–47.
36. Jeffrey SC, Burke PJ, Lyon RP, Meyer DW, Sussman D, Anderson M, et al. A potent anti-CD70 antibody–drug conjugate combining a dimeric pyrrolobenzodiazepine drug with site-specific conjugation technology. Bioconjugate Chem 2013;24:1256–63.
37. Maziasz T, Kadambi VJ, Silverman L, Fedyk E, Alden CL. Predictive toxicology approaches for small molecule oncology drugs. Toxicol Pathol 2010;38:148–64.
38. Richmond A, Su Y. Mouse xenograft models vs GEM models for human cancer therapeutics. Dis Models Mech 2008;1:78–82.
39. Kamath AV.Translational pharmacokinetics and pharmacodynamics of monoclonal antibodies. Drug Discov Today 2016;21–22:75–83.
40. Voskoglou-Nomikos T, Pater JL, Seymour L. Clinical predictive value of the in vitro cell line, human xenograft, and mouse allograft preclinical cancer models. Clin Cancer Res 2003;9:4227–39.

41. Olson H, Betton G, Robinson D, Thomas K, Monro A, Kolaja G, et al. Concordance of the toxicity of pharmaceuticals in humans and in animals. Reg Toxicol Pharmacol 2000;32: 56–67.
42. Wang Y, Probin V, Zhou D. Cancer therapy-induced residual bone marrow injury-Mechanisms of induction and implication for therapy. Curr Cancer Ther Rev 2006;2:271–9.
43. Clark DL, Andrews PA, Smith DD, DeGeorge JJ, Justice RL, Beitz JG. Predictive value of preclinical toxicology studies for platinum anticancer drugs. Clin Cancer Res 1999;5:1161–7.
44. Kennedy DA, Alley SC, Zhao B, Feldman EJ, O'Meara M, Sutherland M. Abstract DDT02-04: SGN-CD33A: Preclinical and phase 1 interim clinical trial results of a CD33-directed PBD dimer antibody-drug conjugate for the treatment of acute myeloid leukemia (AML). Cancer Res 2015;75: DDT02-4-DDT-4.
45. Patel M, Palani S, Chakravarty A, Yang J, Shyu WC, Mettetal JT. Dose schedule optimization and the pharmacokinetic driver of neutropenia. PloS One 2014;9:e109892.
46. Hinrichs MJ, Dixit R. Antibody drug conjugates: nonclinical safety considerations. AAPS J 2015:1–10.